Theory and Observations of Slow-Mode Solitons in Space Plasmas

K. Stasiewicz

Swedish Institute of Space Physics, SE-751 21 Uppsala, Sweden
Space Research Centre, Polish Academy of Sciences, Warsaw, Poland
(Received 19 May 2004; published 17 September 2004)

A generalized model for one-dimensional magnetosonic structures of large amplitude in space plasmas is presented. The model is verified with multipoint measurements on Cluster satellites in the magnetosheath and the boundary layer under conditions of plasma beta (plasma/magnetic pressure) between 0.1–10. We demonstrate good agreement between the model and observations of large amplitude structures and wave trains, which represent increases of magnetic field and plasma density 2–5 times the ambient values, or local decreases (holes) by ∼(50–80)%. Theoretically derived polarization and propagation properties of slow-mode nonlinear structures are also in agreement with *in situ* measurements in space.

We generalize previous models [1,2] of one-dimensional solitons in two-fluid plasma approximation and show that the generalized equations with anisotropic ion pressure provide a good description for slow-mode solitary structures observed in the magnetosheath and other magnetospheric boundary layers by Cluster spacecraft. We find that the magnetosheath, which is a turbulent layer formed downstream of the bow shock in front of the magnetopause, contains a large number of magnetosonic solitary waves with the magnetic field increased (bright solitons) or decreased (dark solitons or holes). Because the multipoint capabilities of Cluster make it possible to determine the velocity of the structures, we were able to experimentally verify not only the spatial shape of the solitons, but also their propagation angles and velocities. Since the magnetosheath contains shocked and thermalized solar wind plasma at strong turbulence, the presented theory and detailed *in situ* measurements of large scale and large amplitude solitons and nonlinear waves are of general interest for other disciplines where strong turbulence and transition between chaos and structure formation is of significance.

The model is based on Hall-MHD equations for low-frequency phenomena in a collisionless plasma [3]

$$Nm_i \frac{d\mathbf{V}}{dt} = \mathbf{J} \times \mathbf{B} - \nabla \cdot \mathbb{P}, \tag{1}$$

$$\frac{1}{eN} \mathbf{J} \times \mathbf{B} = \mathbf{E} + \mathbf{V} \times \mathbf{B}, \tag{2}$$

where N is the number density, m_i is ion mass, $\mathbf{V}$ is velocity, $\mathbf{E}, \mathbf{B}$ are, respectively, electric and magnetic fields, and $\mathbf{J}$ is electric current. The pressure tensor is

$$\mathbb{P} = p_\perp \delta_{ii} + (p_\parallel - p_\perp)\hat{b}_i\hat{b}_j, \tag{3}$$

where $\hat{b}_i$ are components of the unit vector $\mathbf{B}/B$. We assume a general relation for the perpendicular pressure

$$p_\perp = p_{\perp 0}(N/N_0)^\gamma (B/B_0)^\kappa \tag{4}$$

and define a pressure anisotropy parameter

$$a_p = p_\parallel/p_\perp - 1. \tag{5}$$

One-dimensional nonlinear waves are best studied in the stationary wave frame because it is time independent, and in this frame curl$\mathbf{E} = -\partial \mathbf{B}/\partial t = 0$. A structure moving in the x direction, at an angle α to $\mathbf{B}_0 = B_0(\cos\alpha, 0, \sin\alpha)$ with flow velocity $(V_{x0}, 0, 0)$ and the density N_0 at $x = -\infty$ has $B_x = $ const (because div$\mathbf{B} = 0$), and the continuity equation leads to the flux conservation, $NV_x = $ const. In dimensionless form, $\mathbf{b} = \mathbf{B}/B_0$, $V_{x0}/V_x = N/N_0 = n$, the x component of the momentum equation (1) can be integrated and gives

$$2M_A^2(n^{-1} - 1) + \beta(n^\gamma b^\kappa - 1) + b^2 - 1 + b_{x0}^2 a_p \beta(n^\gamma b^{\kappa-2} - 1) = 0, \tag{6}$$

where $\beta = 2\mu_0 p_{\perp 0}/B_0^2$, $M_A^2 = V_{x0}^2/V_A^2$ is the Alfvén Mach number, $V_A^2 = B_0^2/\mu_0 N_0 m_i$, and $b_{x0}^2 = \cos^2\alpha$. The transverse components of the generalized Ohm's law (2) can be cast in the following form:

$$\frac{\lambda_i}{M_x} \frac{\partial b_y}{\partial x} = b_{z0}\left[n - \frac{n}{M_x^2}\left(1 - a_p \frac{\beta}{2}\right)\right]$$
$$- b_z\left[1 - \frac{n}{M_x^2}\left(1 - a_p \frac{\beta}{2} n^\gamma b^{\kappa-2}\right)\right], \tag{7}$$

$$\frac{\lambda_i}{M_x} \frac{\partial b_z}{\partial x} = b_y\left[1 - \frac{n}{M_x^2}\left(1 - a_p \frac{\beta}{2} n^\gamma b^{\kappa-2}\right)\right], \tag{8}$$

where $M_x = M_A/\cos\alpha$, $\lambda_i = V_A/\omega_{ci}$ is the inertial ion length, and the velocities are eliminated with the use of (1). Equations (6)–(8) form a complete system of equations for the spatial dependence of field variables n, b_y, b_z (and other derivables: flows, currents, and electric fields) in terms of the parameters $M_A, \beta, \alpha, \gamma, \kappa$. In the limit $\kappa = 0$, $a_p = 0$ they are equivalent to equations given in [2]. By comparing numerical solutions with observations on Cluster spacecraft we demonstrate that Eqs. (6)–(8) pro-

vide a realistic model for various kinds of magnetosonic structures related to the ion inertial scale length.

The choice of the pressure equation has been a delicate matter when using the fluid equations, with a simple polytropic equation being the usual choice. Our assumption for the pressure model $p_\perp \propto n^\gamma b^\kappa$ is rather general, because it contains various polytropic approximations $\kappa = 0$, as well as a double adiabatic equation $\gamma = 1$, $\kappa = 1$. It is straightforward to use a pressure model with variable anisotropy by using, e.g., Chew-Goldberger-Low equations for the parallel pressure ($p_\parallel \propto n^3 b^{-2}$; see, e.g., [3]). This possibility is rejected because it leads to a strong $\delta n/\delta b$ response, not supported by Cluster observations discussed further. We assume therefore constant pressure anisotropy $a_p \approx$ const, which implies that kinetic instabilities (e.g., ion cyclotron) keep plasma anisotropy at a constant (marginal instability) level.

Equation (6) determines the general dependence between the density n and the magnetic field b. It should hold for arbitrary amplitude structures, also with kinetic effects, provided there is no strong nonlocal dissipation of energy by, e.g., ions with large gyroradius. Figure 1 shows the $b(n)$ relationship computed for cases described further in this Letter, as well as for dark solitons [4] and shocklets [5].

The linear δn response to $(\delta b_y, b_{z0} + \delta b_z)$ perturbations implied by (6) is

$$\delta n \approx \delta b_z D b_{z0}, \qquad (9)$$

where

$$D = \frac{2 + \kappa\beta - (2 - \kappa)a_p\beta b_{x0}^2}{2M_A^2 - \gamma\beta - a_p\gamma\beta b_{x0}^2}. \qquad (10)$$

A critical Mach number $M_{As}^2 = (1 + a_p\cos^2\alpha)\gamma\beta/2$, which corresponds to the zero in the denominator of (10), and to the sonic Mach number equal to 1, separates fast-mode, in-phase ($\delta n/\delta b > 0$) structures in quadrants Q1/Q3 from slow-mode, antiphase ($\delta n/\delta b < 0$) waves and structures in quadrants Q2/Q4. Note that the sonic Mach number can be expressed as $M_s^2 = V_{x0}^2/(\gamma p_0/N_0 m_i) = 2M_A^2/\gamma\beta$.
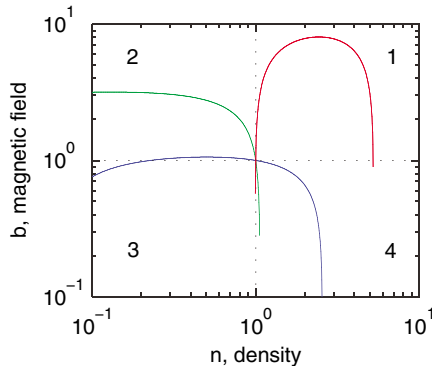
The differential equations (7) and (8) have nonlinear wave solutions with growing amplitudes. The condition for nonlinear waves is found by linearization of Eqs. (6)–(8) around the equilibrium state $n = 1 + \delta n$, $b_y = \delta b_y$, $b_z = b_{z0} + \delta b_z$ and seeking exponentially varying solutions $\propto \exp(x/\lambda)$. This procedure leads to condition

$$\lambda^{-2} = M_x^{-2} A(C - A), \qquad (11)$$

where the nonlinear growth scale λ is in units of λ_i, and

$$A = M_x^2 - 1 + a_p\frac{\beta}{2}, \qquad (12)$$

$$C = b_{z0}^2\left[\left(M_x^2 - \gamma a_p\frac{\beta}{2}\right)D + (2 - \kappa)a_p\frac{\beta}{2}\right]. \qquad (13)$$

Figure 2 shows the location of solitary wave solutions prescribed by $\lambda^2 > 0$ for $\beta = 5$, applicable to the magnetosheath case of Cluster measurements discussed later in this Letter. Figure 3 shows a similar picture for $\beta = 0.5$, which is a typical value for boundary layers inside the magnetopause. Dark magnetosonic solitons reported in [4] correspond to the lower left region of Fig. 3 (low β, small Mach numbers, and quasiperpendicular propagation). A missing factor $(1 - M_x^{-2})$ should appear in front of the right-hand side of Eq. (6) in Ref. [4].

To test the capabilities of the presented model in a high-β regime we apply it to measurements made by Cluster during the bow shock and magnetosheath crossing of 3 February 2002. During this event the four Cluster satellites, separated by $\sim$200 km, were traveling at a speed of 2 km/s toward the Earth, away from the undisturbed solar wind region. They passed through the foreshock (04:00–04:40 UT) and entered the main shock

FIG. 1 (color online). Normalized field b versus density n described by (6) for a number of plasma regimes. Quadrant Q1: fast shocklets ($\beta = 10$, $M_A = 9$). Q2: bright solitons ($\beta = 10$, $M_A = 0.2$), and Q4: dark solitons ($\beta = 0.3$, $M_A = 0.2$). In all cases $\gamma = 1.6$, $\kappa = 0$, and $a_p = 0$.
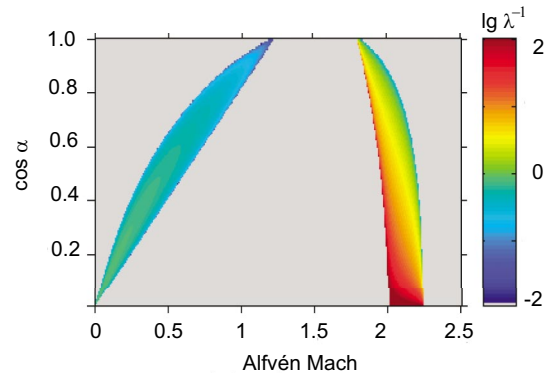
FIG. 2 (color online). Spatial growth rate $\log\lambda^{-1}$ of nonlinear waves for $\beta = 5$, $\gamma = 1.6$, $\kappa = 0$, and $a_p = -0.2$. The vertical border starting at $M_A \approx 2$ corresponds to a singularity at M_{As} which separates slow modes (left) from fast modes (right).
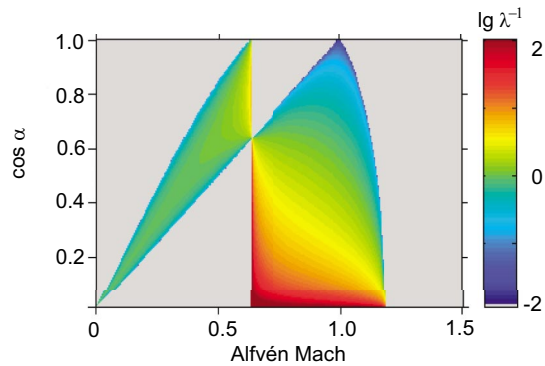
FIG. 3 (color online).   Same as in Fig. 2 for $\beta = 0.5$ and $a_p = 0$. The oblique line corresponds to $A = 0$ in Eq. (11).

region 04:52 UT at a radial distance of $13.5R_E$ and a position of $(10, 3.8, -7.6)R_E$ in geocentric solar ecliptic (GSE) coordinates. The satellites then moved for several hours through the magnetosheath toward the magnetopause layer, before crossing it at 09:15 UT, at the position of $(5, 0, -8)R_E$, GSE. The Cluster satellites encountered during this passage hundreds of large amplitude solitary waves and wave trains. They all appear to be well classified by Fig. 1 in a sense that in the foreshock and the main shock where the solar wind flow is high-β and supersonic, the Cluster observes structures from Q1, which are called shocklets. When the plasma flow slows down below the sonic Mach number 1, the observed structures represent a long series of bright solitons from Q2, and closer to the magnetopause dark solitons or magnetic holes from Q4.

Figure 4 shows an example of a nonlinear wave train measured by Cluster in the magnetosheath. The observed plasma parameters during this event are $V_A \approx 60$ km/s, thermal ion gyroradius about 100 km, $\lambda_i \approx 40$ km, and ion $\beta \approx 10$. The multipoint capabilities of Cluster make it possible to determine the phase velocity of plasma structures by using the time shifts of a structure seen on four Cluster satellites. The data analysis shows that the velocities of the structures in the plasma frame are not negligible (~ 0.1–$0.3V_A$) and have directions quasi-

perpendicular to **B**. There is an ion temperature anisotropy measured by the Cluster ion spectrometer (CIS) [6] of the order $T_{i\perp}/T_{i\parallel} \approx 1.2$–$1.4$ throughout the magnetosheath. This gives an anisotropy parameter $a_p \sim -0.2$. The plasma pressure is dominated by ions ($p_e/p_i \sim 5\%$), and therefore the form of the electron pressure function is not relevant for the momentum balance.
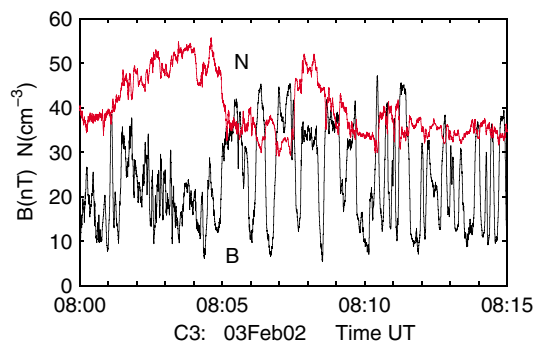
The magnetic field shown in Fig. 4 is sampled at the rate of 22 s^{-1} and provided by the magnetometer team [7]. The electron plasma density is determined from the satellite potential measured by the electric field and wave experiment [8] with sampling rate 5 s^{-1}. It is calibrated with a wide-band receiver that gives the local electron plasma frequency. It agrees also with moments of the ion distribution function determined by CIS (sampled at 0.25 s^{-1}). See Ref. [9] for descriptions of all experiments on Cluster.

A detailed determination of velocities and field polarization is done for one structure at 08:01 UT in Fig. 5, which shows three components of the magnetic field presented in minimum variance coordinates. Determination of the velocity of the structure from the time difference of measurements on the four spacecrafts gives $\mathbf{U} = (-40, -110, 0)$ km/s GSE with an error of 5 km/s. The ion flow determined from the CIS measurements is $\mathbf{V}_i = (-60, -110, 0)$ km/s with an accuracy of 10 km/s. This means that the soliton moves in respect to the plasma with a velocity of 10–20 km/s. Because the Alfvén speed is about 60 km/s, this implies Alfvén Mach number $M_A \approx 0.10$–0.30. The propagation direction with respect to the magnetic field is found by computing the variance matrix of the measured field. The minimum variance (a proxy for $\partial B_x/\partial x = 0$) determines the propagation x-axis direction, which is found to be $\alpha \approx 84° \pm 3°$.

Equations (6)–(8) are solved numerically in the parameter range derived from observations discussed above. The result shown in Fig. 6 is in a reasonable agreement with the measurements. Not only the observed amplitude can be recovered from the governing equations, but also

FIG. 4 (color online).   Cluster measurements of large amplitude magnetosonic structures in the magnetosheath, shown with total magnetic field and plasma density.
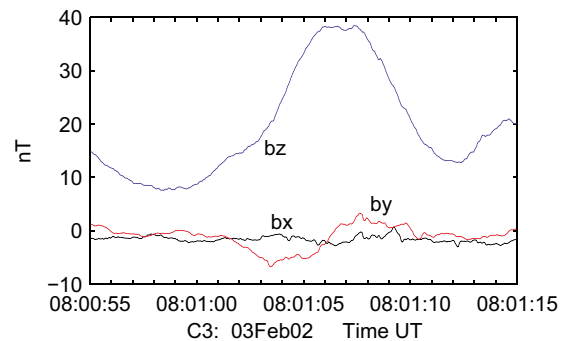
FIG. 5 (color online).   Three-component magnetic field measured on Cluster-3 and displayed in minimum variance coordinates.
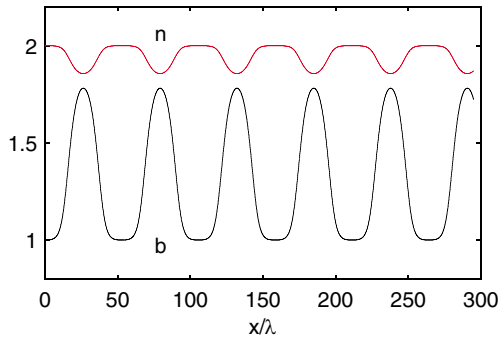
FIG. 6 (color online). A train of solitons obtained as an exact solution of Eqs. (6)–(8) for $\beta = 10$, $M_A = 0.1$, $\alpha = 81.6°$, $\gamma = 1.6$, $\kappa = 0$, and $a_p = -0.1$ (normalized units). The distance of $300\lambda_i$ corresponds to 100 s of Cluster data in Fig. 4.

FIG. 7 (color online). Transverse components of the magnetic field taken from solutions shown in Fig. 6. The solutions resemble Cluster measurements. The distance of $30\lambda_i$ corresponds to 10 s in Fig. 5.

the length scales appear to agree as well. The soliton passes over the spacecraft with a speed of $\sim 3\lambda_i/$s. This means that 1 s of Cluster data corresponds to $3\lambda_i$ in computations.

Polarization of transverse components of the magnetic field is an important property of magnetosonic solitons. Measurements displayed in Fig. 5 are to be compared with the numerical solutions shown in Fig. 7. One can see that the numerical model reproduces well the measured polarization and the spatial size of the soliton. Such a good agreement is related to the inclusion of the pressure anisotropy terms in the governing equations. These terms significantly modify the polarization properties of the solutions (b_y, b_z), which can be nearly linearly polarized as is seen in Fig. 7. Cluster observations of slow-mode structures show predominantly small b_y components, i.e., nearly linear polarization. The soliton solutions obtained previously for the isotropic pressure model [1,2] exhibit generally (b_y, b_z) hodograms with a cardioid shape for bright solitons, with b_y comparable to b_z. The present model with anisotropic pressure provides more flexibility for the solutions and better agreement with observations.

As seen in Fig. 4 there is a rather weak δn response to large magnetic variations δb. It is found that pressure model parameters γ, κ affect strongly the density response to the magnetic field variations. Polytropic models ($\kappa = 0$) with high γ give values of $\delta n / \delta b$ comparable to observations, while other models with $\kappa > 0$ give generally a much stronger response, not supported by measurements. For this reason, $\gamma = 1.6$ and $\kappa = 0$ were adopted in numerical computations.

It should be pointed out that previous observations made on other spacecraft, similar to those presented in Fig. 4, have been described in numerous publications as mirror-mode waves. The solutions shown in this Letter indicate that mirror-mode structures represent robust Hall-MHD effects not necessarily requiring a kinetic
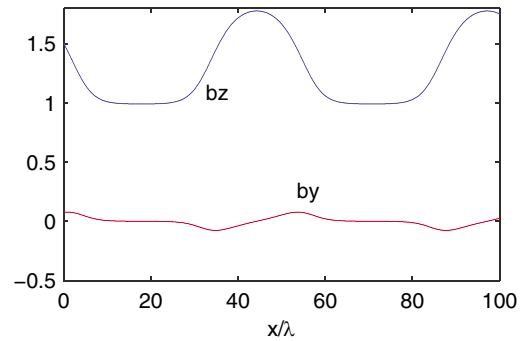
instability. This problem needs further investigation that will be pursued elsewhere.

The fast-mode shocklets have been only briefly mentioned in this Letter. As seen in Fig. 1 (Q1), they exhibit an interesting loop in the $b(n)$ relation, which permits structures with the magnetic field maximum occurring in the middle of the density increase. Such objects are indeed observed, and the first detailed measurements of these structures have been published in [5]. Fast-mode structures from Q3 (depressions of both B and N) have not been identified yet in the Cluster data set.

In summary, this Letter provides some physical bases for a better understanding of large amplitude nonlinear magnetosonic structures in space and astrophysical plasmas and identifies several problems in nonlinear plasma physics that require further investigations.

[1] K. Baumgärtel, J. Geophys. Res. **104**, 28295 (1999).
[2] J. F. McKenzie and T. B. Doyle, Phys. Plasmas **9**, 55 (2002).
[3] N. A. Krall and A. W. Trivelpiece, *Principles of Plasma Physics* (McGraw-Hill, New York, 1973).
[4] K. Stasiewicz, P. K. Shukla, G. Gustafsson, S. Buchert, B. Lavraud, B. Thide, and Z. Klos, Phys. Rev. Lett. **90**, 085002 (2003).
[5] K. Stasiewicz, M. Longmore, S. Buchert, P. Shukla, B. Lavraud, and J. Pickett, Geophys. Res. Lett. **30**, 2241 (2003).
[6] H. Rème *et al.*, Ann. Geophys. **19**, 1303 (2001).
[7] A. Balogh *et al.*, Ann. Geophys. **19**, 1207 (2001).
[8] G. Gustafsson *et al.*, Ann. Geophys. **19**, 1219 (2001).
[9] Special issue of Space Sci. Rev. **79**, Nos. 1–2 (1997).